Structure and dielectric properties of cubic Bi 2 (Zn 1∕3 Ta 2∕3) 2 O 7 thin films

Jun Hong Noh, Hee Beom Hong, Jung-Kun Lee, Chin Moo Cho, Jin Young Kim, Sangwook Lee, In-Sun Cho, Hyun Suk Jung, and Kug Sun Hong

---

Articles you may be interested in

High-temperature dielectric response in pulsed laser deposited Bi 1.5 Zn 1.0 Nb 1.5 O 7 thin films
J. Appl. Phys. **108**, 054106 (2010); 10.1063/1.3457335

Enhanced tunable and pyroelectric properties of Ba (Ti 0.85 Sn 0.15) O 3 thin films with Bi 1.5 Zn 1.0 Nb 1.5 O 7 buffer layers
Appl. Phys. Lett. **96**, 082901 (2010); 10.1063/1.3309419

Effect of excess bismuth concentration on dielectric and electrical properties of fully crystallized Bi 2 Mg 2∕3 Nb 4∕3 O 7 thin films
Appl. Phys. Lett. **91**, 072904 (2007); 10.1063/1.2771381

Structure, dielectric and optical properties of Bi 1.5 ZnNb 1.5 − x Ta x O 7 cubic pyrochlores
J. Appl. Phys. **101**, 104116 (2007); 10.1063/1.2735409

Laser deposition and dielectric properties of cubic pyrochlore bismuth zinc niobate thin films
J. Vac. Sci. Technol. A **24**, 261 (2006); 10.1116/1.2165665

Structure and dielectric properties of cubic Bi$_2$(Zn$_{1/3}$Ta$_{2/3}$)$_2$O$_7$ thin films

Jun Hong Noh,[1] Hee Beom Hong,[1] Jung-Kun Lee,[3,a)] Chin Moo Cho,[1] Jin Young Kim,[4]
Sangwook Lee,[2] In-Sun Cho,[2] Hyun Suk Jung,[5] and Kug Sun Hong[1,2]
[1]*Department of Materials Science and Engineering, Seoul National University, Seoul 151-742, Republic of
Korea*
[2]*Research Institute of Advanced Materials, Seoul National University, Seoul 151-742, Republic of Korea*
[3]*Department of Mechanical Engineering and Materials Science, University of Pittsburgh, Pittsburgh,
Pennsylvania 15260, USA*
[4]*Chemical and Biosciences Center, National Renewable Energy Laboratory, Golden, Colorado 80401, USA*
[5]*School of Advanced Materials Engineering, Kookmin University, Jeongneung-dong, Seongbuk-gu,
Seoul 136-702, South Korea*

Pyrochlore Bi$_2$(Zn$_{1/3}$Ta$_{2/3}$)$_2$O$_7$ (BZT) films were prepared by pulsed laser deposition on Pt/TiO$_2$/SiO$_2$/Si substrates. In contrast to bulk monoclinic BZT ceramics, the BZT films have a cubic structure mediated by an interfacial layer. The dielectric properties of the cubic BZT films [$\varepsilon \sim 177$, temperature coefficient of capacitance (TCC) ~ -170 ppm/°C] are much different from those of monoclinic BZT ceramics ($\varepsilon \sim 61$, TCC $\sim +60$ ppm/°C). Increasing the thickness of the BZT films returns the crystal structure to the monoclinic phase, which allows the dielectric properties of the BZT films to be tuned without changing their chemical composition. © *2009 American Institute of Physics*. [doi:10.1063/1.3246807]

I. INTRODUCTION

The rapid development of wireless communication technologies has led to a need for the miniaturization of components whose performance can be greatly improved by employing novel dielectric materials. The most attractive features of Bi-based pyrochlores are their high dielectric constant and low dielectric loss. Moreover, the temperature stability of their dielectric properties can be easily tuned by controlling their composition.[1] The general chemical formula of oxide pyrochlores can be written as $A_2B_2O_7$ which has two different cation coordinates. While the A-site is filled with trivalent ions with eightfold coordination, the B-site retains tetravalent ions with sixfold coordination.

Recently, the structure and dielectric properties of Bi$_2$(Zn$_{1/3}$Ta$_{2/3}$)$_2$O$_7$ (BZT) have been intensively studied due to its high dielectric constant and interesting low-temperature phase transition.[2–4] BZT ceramics have a distorted pyrochlore structure with a monoclinic symmetry, which is also observed in Bi$_2$(Zn$_{1/3}$Ta$_{2/3}$)$_2$O$_7$ ceramics. This distorted pyrochlore structure of BZT is called the zirconolyte phase and the major difference between the pyrochlore and the zirconolyte phases is the stacking sequence of the tungsten bronze layers. At room temperature, monoclinic BZT ceramics have been reported to show a dielectric constant (ε_r) of 61 and a loss tangent (tan δ) of 0.001 at 1 MHz.[5] The dielectric properties of BZT ceramics do not show significant dependence on the measuring frequency. In the microwave regime, the dielectric constant and temperature coefficient of capacitance (TCC) of monoclinic BZT ceramics are 60.4 and +78 ppm/°C, respectively.[5] The combination of high dielectric constant, low dielectric loss, and small TCC observed in

the BZT ceramics provides a unique opportunity to develop high performance miniaturized microwave components.

In this study, we grew highly textured BZT thin films on (111) Pt using pulsed laser deposition (PLD) and investigated their crystal structures and dielectric properties. It was observed that the interface reaction layer between BZT and the Pt electrode develops a cubic phase which is different from the monoclinic structure of bulk BZT ceramics. Increasing the thickness of the BZT films results in the formation of both cubic and monoclinic phases and provides tunable dielectric properties that are not available in the bulk counterpart.

II. EXPERIMENTAL PROCEDURE

A stoichiometric BZT target was prepared using a conventional mixed oxide method. BZT thin films were grown on a (111)-oriented Pt/TiO$_2$/SiO$_2$/Si substrate (Inostek, Korea) by PLD. A KrF excimer laser ($\lambda = 248$ nm) beam with a pulse repetition rate of 5 Hz was focused on the target to yield an energy density of 2 J/cm^2. All films were deposited at 700 °C under an oxygen partial pressure of 400 mTorr. The thicknesses of the BZT films were controlled to be 193, 250, 373, and 600 nm by changing the deposition time. After the deposition, the films were cooled at an oxygen pressure of 350 Torr without any further thermal treatment.

The crystal structure of the BZT thin films was investigated using x-ray diffraction (XRD) (model MX18HF-SRA, Mac Science Instruments, Japan) and transmission electron microscopy (TEM) (model CM30, Philips, The Netherlands). The chemical composition of the films was determined through electron probe microanalysis (EPMA) (JXA-8900R, JEOL, Japan) on several different points for each sample. To measure their dielectric properties, Pt electrodes (250 μm in diameter) were deposited on top of the BZT films. The di-

a)Author to whom correspondence should be addressed. Electronic mail: jul37@pitt.edu. Tel.: 412-648-3395. FAX: 412-624-8069.
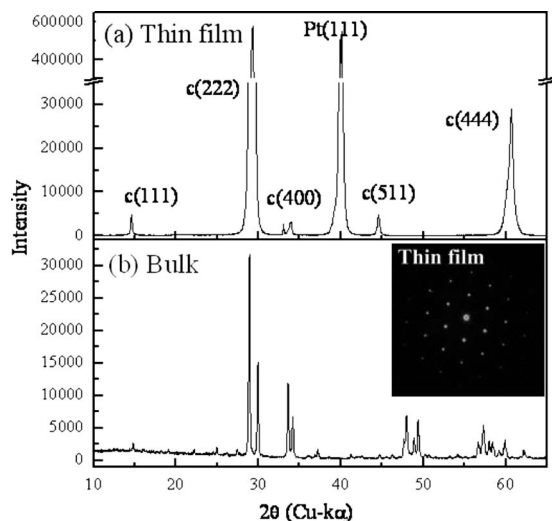
FIG. 1. XRD pattern of (a) the 193-nm-thick $Bi_2(Zn_{1/3}Ta_{2/3})_2O_7$ film on (111)-oriented $Pt/TiO_2/SiO_2/Si$ substrate deposited at 700 °C under an oxygen pressure of 400 mTorr and (b) the bulk $Bi_2(Zn_{1/3}Ta_{2/3})_2O_7$ target. [inset: SAD pattern of TEM along the (111) direction in the $Bi_2(Zn_{1/3}Ta_{2/3})_2O_7$ film].

electric constant (ε_r) and loss (tan δ) of the Pt/BZT/Pt capacitors were measured with an impedance analyzer (HP 4194, Hewlett-Packard, USA) in the range of 100 Hz–10 MHz. The TCC was measured between −20 and 125 °C.

III. RESULTS AND DISCUSSION

Figure 1 shows the XRD pattern of a 193-nm-thick BZT film on a (111)-oriented $Pt/TiO_2/SiO_2/Si$ substrate with a strong ⟨111⟩ preferred orientation. It is noted that no peak split is observed in the XRD pattern of the 193-nm-thick BZT film, indicating that it has a pseudocubic pyrochlore structure. This cubic phase of the PLD-grown BZT films is completely different from the crystal structure of the BZT bulk target. As shown in Fig. 1, the BZT bulk has a monoclinic structure with lattice parameters of $a=13.02$, $b=7.65$, and $c=12.18$ Å, which is consistent with previous studies on the crystal structure of pyrochlore $Bi_2(Zn_{1/3}Ta_{2/3})_2O_7$.[4] The pseudocubic structure of the PLD-grown BZT was confirmed by TEM analysis. The selected area diffraction (SAD) pattern along the ⟨111⟩ direction of the PLD-grown BZT film in the inset of Fig. 1 shows the hexagonal pattern of the cubic or rhombohedral structure without any additional satellite spots. This confirms that it does not have a distorted pyrochlore structure. Given that PLD is very effective in transferring the structure of the parental target materials to the films, this reconstructive phase transition in the PLD-grown BZT film is unusual. The appearance of the cubic phase might be due to the compositional change. In the $Bi_2O_3-ZnO-Ta_2O_5$ ternary system, there is a cubic pyrochlore compound, $(Bi_{1.5}Zn_{0.5})(Zn_{0.5}Ta_{1.5})O_7$. When the A-site of the pyrochlore structure is shared by Bi and Zn, the effect of the $6s^2$ lone pair electrons of Bi on the structural distortion is minimized and the cubic structure is allowed. Therefore, the composition of the cubic BZT film was analyzed using EPMA and compared to that of the target materials. Table I shows that

TABLE I. Compositional analyses of the 193 nm thick $Bi_2(Zn_{1/3}Ta_{2/3})_2O_7$ thin film by EPMA

	Theoretical composition	Measured composition
Bi	50.00	50.19 ± 0.82
Zn	16.67	15.61 ± 0.03
Ta	33.33	34.20 ± 0.83

the composition of the cubic BZT film is almost the same as that of the bulk target, suggesting that the cubic structure in the 193-nm-thick BZT film cannot be attributed to the compositional change during the PLD process. The other possible explanation for the appearance of the cubic phase in the PLD-grown BZT film is lattice matching between BZT and the Pt substrate, which has been widely observed in thin film growth.[6,7] Since the triple of the Pt lattice parameter (3.923 Å) closely matches the lattice parameter of the cubic BZT film (10.561 Å), the cubic BZT structure can be commensurate with that of the (111) Pt bottom electrode with the crystallographic relationship of $(111) [100]_{BZT} \| (111) [100]_{Pt}$. To investigate the effect of the lattice parameter of the substrate, the PLD deposition was performed using the same processing parameters on a (111)-$SrTiO_3$ (STO) substrate whose lattice parameter (3.905 Å) is similar to that of Pt. In contrast to the Pt substrate, the BZT film on (111) STO results in a polycrystalline monoclinic phase without any preferred orientation (not shown here). This indicates that the physical interactions of the deposited atoms with the substrate cannot explain the formation of the cubic phase in the BZT films on (111)-oriented $Pt/TiO_2/SiO_2/Si$ substrates. Recently, we showed that highly (hhh)-oriented pyrochlore $(Bi_{1.4}Zn_{0.6})(Ti_{1.4}Nb_{0.6})O_7$ (BZTN) thin films can be grown on a Pt layer via an interfacial reaction.[8] This is traced to the $Bi_2Pt_2O_7$ interfacial layer that is formed by the preferential reaction of laser-ablated Bi with Pt at 700 °C.[9,10] The interfacial reaction found in our recent study provides an alternative explanation for the formation of the cubic BZT films. The interface between the cubic BZT films and the Pt layer was analyzed using high resolution TEM (HRTEM). The HRTEM image in Fig. 2(b) shows the presence of an inter-
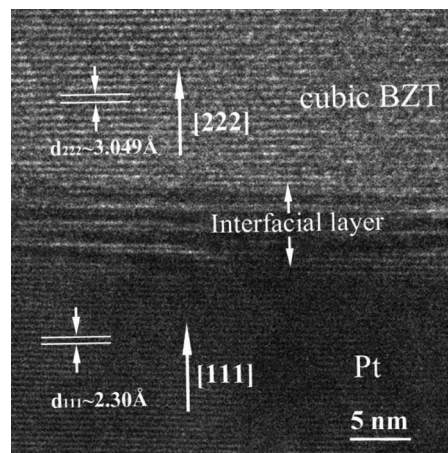

FIG. 2. HRTEM image of thick $Bi_2(Zn_{1/3}Ta_{2/3})_2O_7$ film grown on (111)-oriented $Pt/TiO_2/SiO_2/Si$ substrate.

TABLE II. Dielectric properties of monoclinic and cubic ceramics and 193-nm-thick cubic thin film at 1 MHz.

|	Permittivity ε	Loss $\tan \delta$	TCC (ppm/K)
Monoclinic $Bi_2(Zn_{1/3}Ta_{2/3})_2O_7$ ceramic	61	1.0×10^{-3}	+60
Cubic $(Bi_{1.5}Zn_{0.5})(Zn_{0.5}Ta_{1.5})O_7$ ceramic[a]	74	2.9×10^{-4}	−202
Cubic $Bi_2(Zn_{1/3}Ta_{2/3})_2O_7$ thin film	177	8.0×10^{-3}	−170

[a]See Ref. 11.

facial layer and the growth of the cubic BZT films on top of this layer. This implies that the appearance of the cubic BZT films is mainly due to the formation of thermodynamically stable $Bi_2Pt_2O_7$, which has a cubic structure with a lattice parameter of 10.37 Å that is very close to that of cubic BZT films.

Table II summarizes the dielectric properties of the monoclinic BZT ceramics and cubic BZT films. While the monoclinic BZT ceramics have a positive TCC (+60 ppm/°C) and a dielectric constant of 61, the cubic BZT films exhibit a negative TCC of −170 ppm/°C and a dielectric constant of 177 at 1 MHz. This large difference in their dielectric properties is the other experimental evidence for the cubic phase of the PLD-grown BZT thin films. In contrast to the monoclinic pyrochlore $Bi_2(Zn_{1/3}Ta_{2/3})_2O_7$, the TCC of the cubic pyrochlore $(Bi_{3/2}Zn_{1/2})(Zn_{1/2}Ta_{3/2})O_7$ is negative and its dielectric constant is larger than that of monoclinic $Bi_2(Zn_{1/3}Ta_{2/3})_2O_7$.[11] A similar correlation between the dielectric properties and the crystal structure has been reported in other ternary pyrochlore systems consisting of cubic $(Bi_{3/2}Zn_{1/2})(Zn_{1/2}Nb_{3/2})O_7$ and monoclinic $Bi_2(Zn_{1/3}Nb_{2/3})_2O_7$.[1] This indicates that the crystallographic structure of the pyrochlore phase BZT films significantly affects their dielectric properties. Herein, the dielectric constant of the cubic $Bi_2(Zn_{1/3}Ta_{2/3})_2O_7$ thin film ($\varepsilon \sim 177$) is even higher than that of the cubic $(Bi_{3/2}Zn_{1/2})(Zn_{1/2}Ta_{3/2})O_7$ ($\varepsilon \sim 74$), which might be due to its large total polarizability, as well as its crystal structure. In previous studies, Wang *et al.* showed that the dielectric constant of cubic $(Bi_{3/2}Zn_{1/2})(Zn_{1/2}Nb_{3/2})O_7$ ($\varepsilon \sim 148$) is much higher than that of cubic $(Bi_{3/2}Zn_{1/2})(Zn_{1/2}Ta_{3/2})O_7$ ($\varepsilon \sim 74$) because the higher polarizability of Nb increases the total polarizability of the unit cell.[11] In addition, according to Shannon's report, ion dielectric polarizabilities of Bi, Zn, and Ta given in Å³ are 6.12, 2.04, and 4.73, respectively.[12] In this study, therefore, the unit cell of the cubic $Bi_2(Zn_{1/3}Ta_{2/3})_2O_7$ film has higher total ion polarizability than that of the cubic $(Bi_{3/2}Zn_{1/2})(Zn_{1/2}Ta_{3/2})O_7$ bulk since the higher ratio of Bi ion in the *A*-site of $Bi_2(Zn_{1/3}Ta_{2/3})_2O_7$ increases the total polarizability of the unit cell. Therefore, the high dielectric constant of the cubic $Bi_2(Zn_{1/3}Ta_{2/3})_2O_7$ films is attributed to their distortion-free cubic structure and high ionic polarizability.

Figure 3 shows the effect of the film thickness on the structure of the BZT films. As the film thickness increases, a peak split is observed in the (444) reflection. The new peak of the 600-nm-thick BZT film corresponds to the monoclinic (442) reflection, indicating that the increase in the film thickness allows the coexistence of the cubic and monoclinic
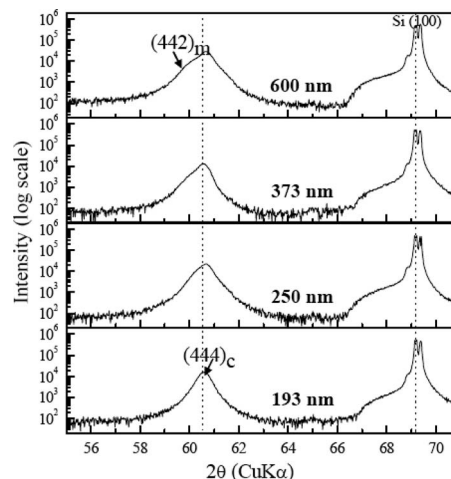
FIG. 3. XRD profiles of the $Bi_2(Zn_{1/3}Ta_{2/3})_2O_7$ thin film with various film thickness (m: monoclinic phase, c: cubic phase).

phases. Figure 4 quantitatively shows the internal stress of the films calculated using the measured sample curvature and Stoney relations.[13] The in-plane tensile stress decreases as the film thickness increases up to 600 nm. At a film thickness of 373 nm, at which the monoclinic phase coexists with the cubic phase, the in-plane tensile stress is drastically decreased by 300 MPa. The plane-view TEM micrograph of the 193-nm-thick BZT film in the inset of Fig. 4 confirms the presence of internal stress in the thinner BZT films. In the TEM micrograph of Fig. 4, a contrast due to a strain field is clearly observed along the grain boundaries of the films. The strain field at the grain boundaries indicates that a certain level of internal stress is present in the 193-nm-thick BZT film,[14,15] which is consistent with the curvature measurement. The tensile stress in the 193-nm-thick BZT film is attributed to the fact that the thermal expansion coefficient of the Si substrate is smaller than that of the Bi-based pyrochlore materials.[16,17] As the film thickness increases, the cubic BZT films mediated by the interfacial layer may not tolerate the increase in the internal stress, and growth defects such as misfit dislocations may start to form in the BZT films. Consequently, the BZT films lose their structural cor-
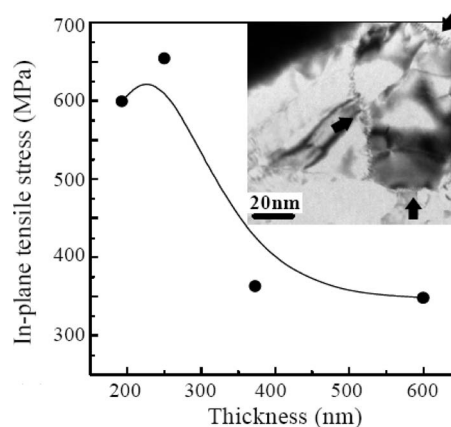
FIG. 4. In-plane tensile stress of $Bi_2(Zn_{1/3}Ta_{2/3})_2O_7$ films as a function of film thickness (inset: plane-view micrograph of TEM for 193-nm-thick $Bi_2(Zn_{1/3}Ta_{2/3})_2O_7$ film with arrows marking a strain field).
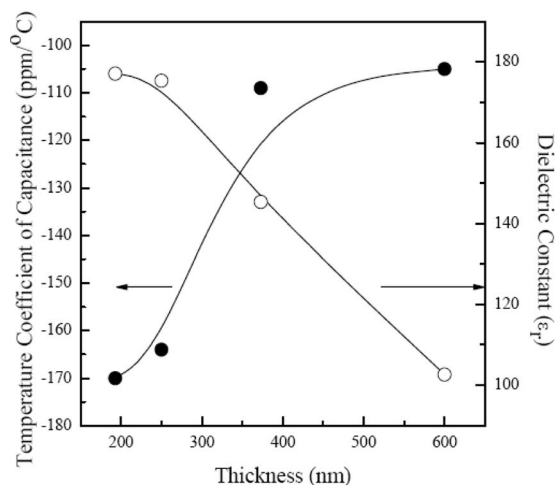
FIG. 5. Dielectric constant (ε_r) and TCC as a function of the film thickness.

relation with the interfacial layer, $Bi_2Pt_2O_7$, and a thermodynamically stable monoclinic phase appears, as shown in Fig. 4.[18,19]

Figure 5 shows the dielectric properties of the films versus their thickness. As the film thickness increases, the TCC increases to -105 ppm/$°$C and the dielectric constant decreases to 103. The change in the dielectric properties in Fig. 5 can be explained by the mixture rule. As the thickness increases, the BZT films partially recover their monoclinic phase that is inherent to the BZT bulk (Fig. 4). Therefore, the negative TCC and high ε_r of the cubic phase are compensated by the positive TCC (60 ppm/$°$C) and low ε_r (61) of the monoclinic phase, leading to the increase in the TCC and decrease in ε_r. This indicates that the dielectric properties of the BZT films can be effectively tuned simply by changing their thickness without altering either their chemical composition or processing parameters, which would be useful in practical applications.

IV. CONCLUSIONS

The structure and dielectric properties of PLD-grown BZT films on (111)-oriented $Pt/TiO_2/SiO_2/Si$ substrates were investigated. In contrast to their bulk counterpart, the BZT films thinner than 200 nm possess a cubic pyrochlore phase and show a high dielectric constant (177) and negative

TCC (-170 ppm/$°$C) at 1 MHz. The change in the dielectric properties of the cubic BZT films is attributed to their higher polarizability and distortion-free cubic structure. The original monoclinic phase gradually reappears as the thickness of the film is increased. The dielectric constant and TCC of the BZT films can be tuned by adjusting their thickness due to the mixture behavior of the two phases.

[1]W. Ren, S. Trolier-McKinstry, C. A. Randall, and T. R. Shrout, J. Appl. Phys. **89**, 767 (2001).
[2]H.-J. Youn, C. A. Randall, A. Chen, T. R. Shrout, and M. T. Lanagan, J. Mater. Res. **17**, 1502 (2002).
[3]I. Levin, T. G. Amos, J. C. Nino, T. A. Vanderah, I. M. Reaney, C. A. Randall, and M. T. Lanagan, J. Mater. Res. **17**, 1406 (2002).
[4]H. B. Hong, D. W. Kim, and K. S. Hong, Jpn. J. Appl. Phys., Part 1 **42**, 5172 (2003).
[5]C. Ang, Z. Yu, H. J. Youn, C. A. Randall, A. S. Bhalla, L. E. Cross, and M. Lanagan, Appl. Phys. Lett. **82**, 3734 (2003).
[6]W.-R. Liu, Y.-H. Li, W. F. Hsieh, C.-H. Hsu, W. C. Lee, Y. J. Lee, M. Hong, and J. Kwo, Cryst. Growth Des. **9**, 239 (2009).
[7]J. Narayan and B. C. Larson, J. Appl. Phys. **93**, 278 (2003).
[8]J. Y. Kim, J. H. Noh, S. Lee, S.-H. Yoon, C. M. Cho, K. S. Hong, H. S. Jung, and J.-K. Lee, Appl. Phys. Lett. **91**, 232903 (2007).
[9]M. L. Calzada, A. Gonzalez, J. García-Lopez, and R. Jimenez, Chem. Mater. **15**, 4775 (2003).
[10]Y. Shimakawa and Y. Kubo, Appl. Phys. Lett. **75**, 2839 (1999).
[11]Q. Wang, H. Wang, and X. Yao, J. Appl. Phys. **101**, 104116 (2007).
[12]R. D. Shannon, J. Appl. Phys. **73**, 348 (1993).
[13]G. G. Stoney, Proc. R. Soc. London, Ser. A **82**, 172 (1909).
[14]J. K. Lee and K. S. Hong, J. Am. Ceram. Soc. **84**, 2001 (2001).
[15]D. Jawarani, H. Kawasaki, I. S. Yeo, L. Rabenberg, J. P. Stark, and P. S. Ho, J. Appl. Phys. **82**, 1563 (1997).
[16]H. Funakubo, S. Okaura, M. Suzuki, H. Uchida, S. Koda, R. Ikariyama, and T. Yamada, Appl. Phys. Lett. **92**, 182901 (2008).
[17]J. Lu, D. O. Klenov, and S. Stemmer, Appl. Phys. Lett. **84**, 957 (2004).
[18]P. Werner, N. D. Zakharov, Y. Chen, Z. Liliental-Weber, J. Washburn, J. F. Klem, and J. Y. Tsao, Appl. Phys. Lett. **62**, 2798 (1993).
[19]H. J. Kim, S. H. Oh, and H. M. Jang, Appl. Phys. Lett. **75**, 3195 (1999).